PUFFIN: A THREE DIMENSIONAL, UNAVERAGED FREE ELECTRON LASER SIMULATION CODE

L.T. Campbell and B.W.J. McNeil

SUPA, Department of Physics, University of Strathclyde, Glasgow, UK

Abstract

The broadband, 3D FEL code Puffin is presented. The analytical model is derived in absence of the Slowly Varying Envelope Approximation, and can model undulators of any polarization. Due to the enhanced resolution, the memory and processing requirements are greater than equivalent averaged codes. The numerical code to solve the system of equations is therefore written for a parallel computing environment utilizing MPI. An example simulation is presented.

INTRODUCTION

Most analytical and numerical models of the FEL use the Slowly Varying Envelope Approximation [1] (SVEA) on the radiation field. This assumes a slow temporal and spatial evolution of the field envelope at the scale of the radiation wavelength, and allows an averaging of the field envelope and some electron phase-space parameters over at least one radiation period, removing the need to model any fast oscillatory terms at the radiation frequency. Most of the commonly used multi-dimensional FEL simulation codes (e.g. MEDUSSA [2], GINGER [3], GENESIS 1.3 [4] and FAST [5]), are based on averaged SVEA models. While these have been used successfully to model basic FEL operation, and have been extensively benchmarked against experiment, SVEA means that resolution of sub-resonant wavelength scale processes are not possible. The particles used to simulate the electrons are confined to localised regions of one radiation period within the electron pulse, so that transport of particles over many radiation wavelengths, such as may occur as a result of the FEL interaction or e.g. a pre-imposed electron energy chirp, cannot be modelled easily. Furthermore, the correct simulation of electron shot-noise is only valid for a limited radiation wavelength range [6]. The minimum sampling period of the field envelope imposed by SVEA also limits the range of radiation frequencies able to be modelled without numerical aliasing effects to $\omega_r/2 < \omega < 3\omega_r/2$, where ω_r is the radiation resonant frequency [7]. Thus, using SVEA, it is not possible to model effects with a broader bandwidth using the same radiation field envelope. Such issues with SVEA constrain the effective modelling of several more advanced FEL methods including designs to achieve shorter radiation wavelengths and pulse durations [8].

This paper presents what the authors believe to be the first 3D unaveraged, broadband FEL computer simulation code, named Puffin (Parallel Unaveraged Fel INtegrator).

The primary aim of this code is to provide a flexible research resource that can be adapted to test new ideas and methods for future FEL development. It is not intended, at least initially, as a design tool for FEL facility development.

The radiation field is modelled using the Finite Element method [9] and the electrons by a distribution of charge weighted macroparticles that can model the effects of electron shot-noise across a broad frequency bandwith [6]. Electrons are not confined to localised regions of the beam so that electron transport throughout the beam is correctly modelled. The main approximations applied are the neglect of the backward (counterpropagating) radiation field and the paraxial approximation. Furthermore, space-charge effects in the electron beam are neglected.

The resulting parallelised numerical code is able to simulate both CSE and spontaneous emission arising from electron shot-noise. The advantages are an enhanced and broadband resolution of the radiation including a self-consistent modelling of variable radiation polarisation. The disadvantages are the increased computer memory requirements and processing time when compared to the averaged numerical models.

In the following, the derivation of the final working equations and subsequent numerical solution is outlined and the operation of the code is demonstrated using different FEL configurations.

MATHEMATICAL MODEL

The electromagnetic field is given by:

$$\mathbf{E} = \frac{1}{\sqrt{2}} \left(\hat{\mathbf{e}}\xi_0 e^{i(k_r z - \omega_r t)} + c.c. \right), \qquad (1)$$

where the vector basis

$$\hat{\mathbf{e}} = \frac{1}{\sqrt{2}}(\hat{\mathbf{x}} + i\hat{\mathbf{y}}) \qquad (2)$$

and $\xi_0(x,y,z,t) = |\xi_0(x,y,z,t)| \exp(i\psi(x,y,z,t))$ is the complex field envelope, with k_r and ω_r, the field wavenumber and angular frequency respectively, of a resonant wave.

It is assumed the field propagates in vacuum and that the paraxial approximation applies, so that $\omega_r = ck_r$ and $\partial/\partial z \approx \partial/c\partial t$.

The undulator magnetic field is defined as:

$$\mathbf{B}_u = \frac{B_u}{2} \left(\mathbf{u} e^{ik_u z} + c.c. \right) \qquad (3)$$

where $k_u = 2\pi/\lambda_u$ is the undulator wavenumber, λ_u is the undulator wavelength and B_u is the peak magnetic field

of the undulator and the (generally non-unit) vector basis is $\mathbf{u} = (u_x\hat{\mathbf{x}} + iu_y\hat{\mathbf{y}})$. The undulator polarisation is then determined by u_x and u_y, which are the relative peak magnetic undulator field in x or y.

The FEL or Pierce parameter determines the strength of the radiation/electron coupling in the 1-Dimensional limit and is given by [10] $\rho = (\bar{a}_u\omega_p/4ck_u)^{2/3}/\gamma_r$. Here, e and m are the charge magnitude and rest-mass of an electron, c is the speed of light, $\omega_p = \sqrt{e^2n_p/\epsilon_0 m}$ is the (non-relativistic) electron beam plasma frequency, n_p is the peak electron number density, $\bar{a}_u = e\bar{B}_u/mck_u$ is the RMS undulator parameter and γ_r is the electron energy in units of the rest-mass energy corresponding to the resonant FEL wavelength λ_r.

Starting from the coupled Maxwell-Lorentz equations, using the definitions of electromagnetic and undulator fields and above, and defining dimensionless scaled variables:-

$$p_{2j} = \frac{1-\beta_{zj}}{\eta\beta_{zj}}, \qquad \eta = \frac{1-\bar{\beta}_z}{\bar{\beta}_z},$$

$$\bar{p}_\perp = \frac{u}{\sqrt{2}mc\bar{a}_u}p_\perp, \qquad A_\perp = \frac{eu\bar{a}_u l_g}{2\sqrt{2}\gamma_r^2 mc^2\rho}E_\perp,$$

$$\bar{z} = 2k_u\rho z, \qquad \bar{z}_2 = 2k_u\rho\frac{\bar{\beta}_z(ct-z)}{(1-\bar{\beta}_z)},$$

$$\bar{x},\bar{y} = \frac{x,y}{\sqrt{l_g l_c}},$$

where $u^2 = \mathbf{u}\cdot\mathbf{u}^*$, $l_c = 1/2\rho k_r$, and $l_g = 1/2\rho k_u$, gives the final set of working equations as solved numerically by the code:

$$\left[\frac{1}{2}\left(\frac{\partial^2}{\partial\bar{x}^2} + \frac{\partial^2}{\partial\bar{y}^2}\right) - \frac{\partial^2}{\partial\bar{z}\partial\bar{z}_2}\right]A_\perp =$$
$$-\frac{1}{\bar{n}_p}\frac{\partial}{\partial\bar{z}_2}\sum_{j=1}^N\bar{p}_{\perp j}L_j\delta^3(\bar{x}_j,\bar{y}_j,\bar{z}_{2j}) \tag{4}$$

$$\frac{d\bar{p}_{\perp j}}{d\bar{z}} = \frac{1}{2\rho}\left[iU^* - \frac{\eta p_{2j}}{f^2\bar{k}_\beta^2}A_{\perp j}\right] - \frac{u\sqrt{\eta}}{2\sqrt{2}f\bar{k}_\beta\rho L_j}\times$$
$$\left(\bar{k}_\beta^2(\bar{x}_j - i\bar{y}_j) + \frac{\eta}{(1+\eta p_{2j})}\left(\frac{d\bar{x}_j}{d\bar{z}} - i\frac{d\bar{y}_j}{d\bar{z}}\right)\frac{dp_{2j}}{d\bar{z}}\bigg|_F\right) \tag{5}$$

$$\frac{dp_{2j}}{d\bar{z}} = \frac{2\rho}{u^2\eta}L_j^2\left[\eta p_{2j}(A_{\perp j}^*\bar{p}_{\perp j} + c.c.)\right.$$
$$\left. - i(1+\eta p_{2j})f^2\bar{k}_\beta^2(U\bar{p}_{\perp j} - c.c.)\right] + \frac{dp_{2j}}{d\bar{z}}\bigg|_F \tag{6}$$

$$\frac{d\bar{z}_{2j}}{d\bar{z}} = p_{2j} \tag{7}$$

$$\frac{d\bar{x}_j}{d\bar{z}} = \frac{2\sqrt{2}f\bar{k}_\beta\rho}{u\sqrt{\eta}}L_j\Re(\bar{p}_{\perp j}) \tag{8}$$

$$\frac{d\bar{y}_j}{d\bar{z}} = -\frac{2\sqrt{2}f\bar{k}_\beta\rho}{u\sqrt{\eta}}L_j\Im(\bar{p}_{\perp j}). \tag{9}$$

Here, $\bar{n}_p = l_g l_c^2 n_p$ is the peak electron number density at the start of the interaction in the scaling of $(\bar{x},\bar{y},\bar{z}_2)$, $U(\bar{z}) = (u_x\cos(\bar{z}/2\rho) + iu_y\sin(\bar{z}/2\rho))$, and

$$L_j \equiv \frac{\gamma_r}{\beta_{zj}\gamma_j} = \gamma_r\sqrt{\frac{\eta p_{2j}(2+\eta p_{2j})}{1+2\frac{\bar{a}_u^2}{u^2}|\bar{p}_{\perp j}|^2}} \tag{10}$$

The equations (7..9) for the $\bar{z}$-dependent electron coordinates $(\bar{x}_j,\bar{y}_j,\bar{z}_{2j})$ are simply derived from the scaled momentum-energy relations.

The scaled betatron wavenumber is given by $\bar{k}_\beta = \bar{a}_u/2f\rho\gamma_r$, where the scaling is with respect to that of 'natural' undulator focusing [11], when $f = \sqrt{2}$. For variable f the external focusing may be artificially strengthened or weakened. However, the undulator magnetic field (3) has no transverse variation and so natural focussing is not included in the model. Thus the term:

$$\frac{dp_{2j}}{d\bar{z}}\bigg|_F = -\bar{k}_\beta^2\frac{(1+\eta p_{2j})\left(\bar{x}_j\frac{d\bar{x}_j}{d\bar{z}} + \bar{y}_j\frac{d\bar{y}_j}{d\bar{z}}\right)}{1+\eta\left(\left(\frac{d\bar{x}_j}{d\bar{z}}\right)^2 + \left(\frac{d\bar{y}_j}{d\bar{z}}\right)^2\right)}. \tag{11}$$

must be added in equations (5,6), to ensure the electron energy remains constant over betatron period in the absence of a radiation field.

The field equation (4) is derived by neglecting the backwards wave component of the radiation field [12]. In the $1D$ Compton limit, ignoring focusing and diffraction terms, equations (4-7) reduce to those of [6].

In scaled units the Rayleigh range for a Gaussian beam of width of σ_{xr} is $\bar{z}_R = k_r\sigma_{xr}^2/l_g$ which, in the transverse scaling above, may be written $\bar{z}_R = \bar{\sigma}_{xr}^2/2\rho$. By definition, $\bar{z}_R = \pi F$ where F is the Fresnel number for a gain length. For the case of a matched beam, so that the emittance $\epsilon = k_\beta\sigma_{xb}^2$, where σ_{xb} is the (constant) radius of the electron beam and assuming the radiation beam radius is that of the electron beam, the scaled Rayleigh range may be written: $\bar{z}_R = \bar{\epsilon}/2\bar{k}_\beta$ where, the scaled electron beam emittance $\bar{\epsilon} \equiv 4\pi\epsilon/\lambda_r$. Hence, the usual FEL emittance criterion becomes: $\bar{\epsilon} = 2\bar{k}_\beta\bar{z}_R \lesssim 1$

All variables above have been scaled with respect to parameters in the 1D limit. The work of [13] defines a set of 3D scaled parameters: the FEL parameter $\rho_{3D} = B^{1/3}\rho$, where $B = (2\bar{z}_R)^{3/2}$ is called as the 'diffraction parameter'. The scaling can be related to that used here via '1D' Rayleigh range $\bar{z}_R$ by $B = (2\bar{z}_R)^{3/2}$. In a similar way to the 1D scaling a 3D gain length was defined as $\tilde{l}_g = \lambda_u/4\pi\rho_{3D}$ so that the diffraction parameter $B = 2z_R/\tilde{l}_g$.

If the working equations of (4..9) above are scaled with respect to ρ_{3D}, i.e. the substitution $\rho = \rho_{3D}/\sqrt{2\bar{z}_R}$ is made into all dependent and independent variables and these variables redefined so that $\tilde{z} = 2k_u\rho_{3D}z$ etc., then all equations remain identical in form (i.e. with 'bars' replaced by 'tildes' in the independent variables), with the exception of the wave equation (4) which is slightly modified to become:

$$\left[\frac{1}{2}\left(\frac{\partial^2}{\partial\tilde{x}^2} + \frac{\partial^2}{\partial\tilde{y}^2}\right) - \frac{\partial^2}{\partial\tilde{z}\partial\tilde{z}_2}\right]\tilde{A}_\perp =$$
$$-\frac{1}{B\tilde{n}_p}\frac{\partial}{\partial\tilde{z}_2}\sum_{j=1}^{N}\tilde{p}_{\perp j}L_j\delta^3(\tilde{x}_j,\tilde{y}_j,\tilde{z}_{2j}). \quad (12)$$

The 3D FEL parameter ρ_{3D} is then dependent only upon the longitudinal electron current, and the transverse behaviour becomes explicit in the equations via the B parameter. For a constant ρ_{3D}, increasing the transverse radius reduces the transverse electron density, increasing B and reducing the field source and generation.

The numerical implementation in Puffin uses the equations written in terms of the 1D scaling (4-9), mainly to allow easy comparison with 1D simulations and analysis. As has been shown, solutions in the 3D scaling of [13] are simply obtained using the relations discussed above.

NUMERICAL SOLUTION

The parallel numerical algorithm used for the solution of the working equations (4..9) has been developed from [14, 15, 16]. The coupled equations are advanced in $\bar{z}$ by using the split-step Fourier method [17], in which the radiation field is described by the method of finite elements [9] and the electrons are simulated by a distribution of charge weighted macroparticles [6].

Puffin is written in FORTRAN 95, and uses the libraries FFTW 2.1.5 [18], used for the Fourier transforms, and SuperLU_DIST [19, 20] to solve the sparse linear system of equations for the finite element description of the driven wave equation. The initial electron beam and radiation field parameters are read in from an input data file, and in the future it is possible that Puffin will be modified to read in an electron beam distribution output by an external accelerator code. Data output is in the SDDS format [21], and the post-processing in the following examples is performed using MATLAB. The code is parallelized using MPI [22] in a method outlined in [12], and more detail will be given in [23].

SIMULATION

In this section, a full 3D simulation demonstrating Self Amplified Coherent Spontaneous Emission is presented.

An electron beam with a 'top-hat' current distribution of 6 cooperation lengths long in $\bar{z}_2$ and a Gaussian current distribution in $\bar{x}$ and $\bar{y}$, is propagated through an undulator of scaled length $\bar{z} = 8$ using the following parameters:

$\rho = 5.56 \times 10^{-3}, \bar{\epsilon} = 0.6, \bar{a}_u = 1.0, \sigma_{p2} = 0.002, \gamma_r = 700, u_x = u_y = 1$ and $f = \sqrt{2}$.

The top-hat electron pulse should emit strong coherent radiation from its head and tail which have large current gradients. In this high slippage/short pulse regime, the coherent emission from the rear of the electron pulse will propagate through the electron pulse and be amplified. CSE from the tail at the start of the undulator will propagate through and be amplified by the whole of the electron pulse by the end of the undulator.

The electron beam of scaled emittance $\bar{\epsilon} = 0.6$ is matched to the focusing channel with betatron wavenumber $\bar{k}_\beta \approx 0.09$. These parameters give a scaled Rayleigh range ($\bar{z}_R = z/l_g$) of $\bar{z}_R \approx 3.3$.

The simulation results are shown in Figure 1 at propagation distances $\bar{z} \approx 4$ and $\bar{z} \approx 8$. The scaled power P and the transverse intensity distribution $I_\perp$ are plotted at two fixed points in $\bar{z}_2$ for each propagation distance.

In the earlier plots through the interaction, at $\bar{z} \approx 4$, the electron pulse lies between $4 < \bar{z}_2 < 10$. The radiation between $0 < \bar{z}_2 < 4$ is the CSE from the front edge of the electron pulse, having propagated forward into free space. The region from $6 < \bar{z}_2 < 10$ is in the 'slippage region', and here the CSE emitted by the rear of the electron pulse has begun to be amplified. The steady-state region $4 < \bar{z}_2 < 6$, has an evolution dominated by electron shot-noise as seen from the transverse plot of the intensity within this region which still has a poor spatial coherence. In contrast, the intensity near the peak of the amplified CSE demonstrates a good spatial coherence.

Later in the interaction, at $\bar{z} \approx 8$, greater field amplification via the FEL interaction is observed. The electron pulse now lies between $8 < \bar{z}_2 < 14$, and the system is dominated by CSE emitted from the tail of the electron pulse at $\bar{z}_2 = 14$, propagating through and being amplified by the electron pulse. The intensity at $\bar{z}_2 = 4.7$, which previously exhibited poor spatial coherence, now has a good spatial coherence. This is not due only to the onset of the SASE transverse mode selection process, but is also due to the initial noisy spontaneous emission being dominated by the amplified CSE. The scaled intensity plotted near the peak of the amplified radiation pulse, at $\bar{z}_2 = 11.8$, is more narrowly focused than that at $\bar{z}_2 = 4.7$, which has undergone a greater free space diffraction having propagated outside of the electron pulse.

CONCLUSION

The FEL simulation code Puffin has been presented. This is the first code which includes 3D modelling of the radiation field and electron beam using an unavaraged system of equations in a variably polarised, modular undulator. The equations allow a broad bandwidth of radiation frequencies up to a high harmonic of the resonant frequency to be modelled using a single complex field variable. While a relatively simple electron beam focusing channel has been implemented, a more realistic FODO-type focusing lattice
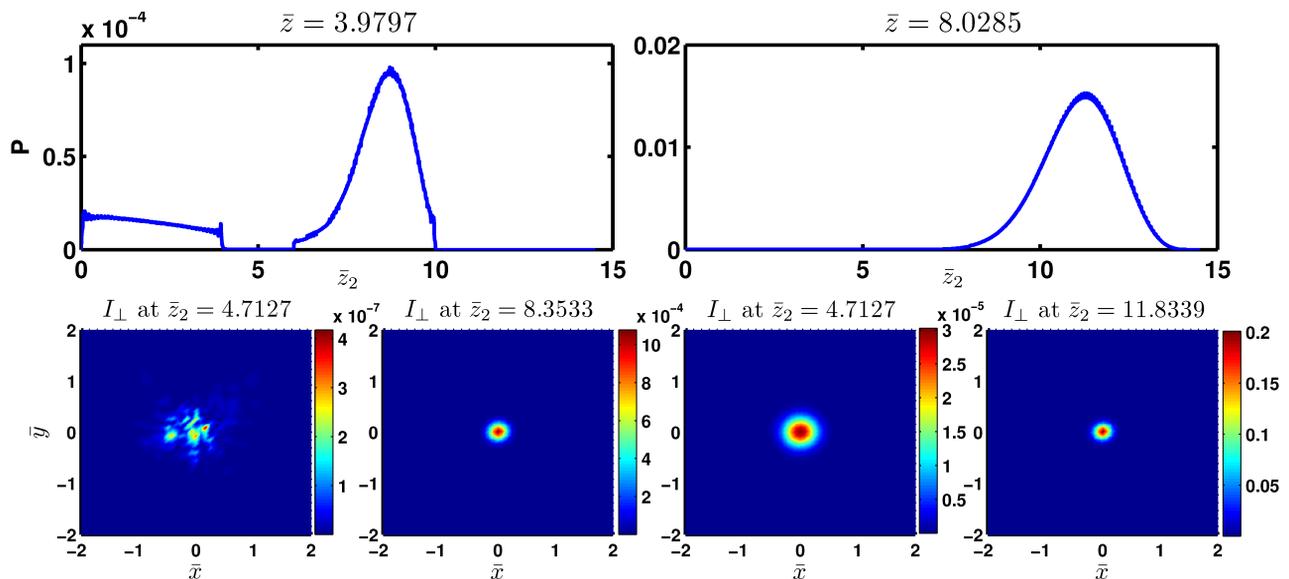
Figure 1: Upper plots: Scaled power $P(\bar{z}_2)$ - the scaled intensity integrated over the transverse plane $(\bar{x}, \bar{y})$, as a function of window scaled position $\bar{z}_2$ for two propagation distances $\bar{z} \approx 4$ and 8. Lower plots: Transverse slices of the scaled intensity $I_\perp(\bar{x}, \bar{y})$ at different window positions in $\bar{z}_2$ with propagation distances corresponding to the upper power plots.

could be included by placing quadrupoles between undulator modules, and modelling the variation in off-axis undulator field components. Future work should also involve the post-processing of data files which is currently not perfomed in parallel. The output data files are also too large to be easily portable and would benefit from being analysed 'on-site' using local visualisation servers. These issues are currently being reviewed.

REFERENCES

[1] F.T. Arecchi and R. Bonifacio, IEEE J. Quantum Electron. **QE-1**, 169 (1965).

[2] H.P. Freund, Phys. Rev. E, **52**, 5401 (1995).

[3] W.M. Fawley, Proceedings of FEL 2006, BESSY, Berlin, Germany, 218-221 (2006).

[4] S. Reiche, Nucl. Instr. and Meth. in Phys. Res. A **429**, 243-248 (1999).

[5] E.L. Saldin *et al*, Nucl. Instr. and Meth. in Phys. Res. A **429**, 233-237 (1999).

[6] B.W. J. McNeil, M.W. Poole and G.R.M. Robb, Phys. Rev. ST AB **6**, 070701 (2003) .

[7] B.W.J. McNeil, J.A. Clarke, D.J. Dunning, G.J. Hirst, H.L. Owen, N.R. Thompson, B. Sheehy and P.H. Williams, New Journal of Physics **9**, 82 (2007).

[8] S. Reiche, *FEL Simulations: History, Status and Outlook*, Proceedings of FEL2010, Malmö, Sweden **MOOCI1**, 165-172 (2010)

[9] K.H. Huebner, E.A Thornton and T.G. Byrom, *The Finite Element Method For Engineers*, (1995) Wiley.

[10] R. Bonifacio, C. Pellegrini and L.M. Narducci, Opt. Comm. **50**, 373 (1984).

[11] E.T. Scharlemann, J. Appl. Phys. **58**, 2154 (1985).

[12] L.T. Campbell and B.W.J. McNeil, *An Unaveraged Computational Model of a Variably Polarized Undulator FEL*, MOPB30, Proceedings of FEL 2010, Malmo, Sweden (2010)

[13] E.L. Saldin, E.A Schneidmiller and M.V. Yurkov, New Journal of Phyics **12**, 035010 (2010).

[14] C.K.W. Nam, *On the Theory and Modelling of the Fourth Generation Light Source*, PhD Thesis, University of Strathclyde, 2009.

[15] C.K.W. Nam, P. Aitken and B.W.J. McNeil, *Unaveraged Three Dimensional Modelling of the FEL*, Proceedings of FEL 2008, Gyeongju, Korea, 2008.

[16] L.T Campbell, *The Physics of a 4th Generation Light Source*, PhD Thesis, University of Strathclyde, 2011.

[17] R.H. Hardin and F.D. Tappert, SIAM Review **15**, 423 (1973).

[18] M. Frigo and S.G. Johnson, *FFTW 2.1.5 Manual*, available from http://www.fftw.org, 2003.

[19] X.S. Li and J.W. Demmel, *SuperLU_DIST: A Scalable Distributed-Memory Sparse Direct Solver for Unsymmetric Linear Systems*, ACM Trans. Mathematical Software, Vol 29, **2**, 110-140 (2003).

[20] L. Grigori, J.W. Demmel and X.S. Li, *Parallel Symbolic Factorization for Sparse LU with Static Pivoting*, SIAM J. Scientific Computing, Vol 29 **3**, 1289-1314 (2007).

[21] M. Borland, A Self-Describing File Protocol for Simulation Integration and Shared Postprocessors, in *Proceedings of the 1995 Particle Accelerator Conference*, May 1-5, 1995, Dallas, Texas, 1995.

[22] P.S. Pacheco, *Parallel Programming with MPI*, Morgan Kaufmann Publishers, Inc., 1997.

[23] L.T. Campbell and B.W.J. McNeil, Submitted to Physics of Plasmas.